Research Paper https://doi.org/10.7733/jnfcwt.2022.001

Surface Modification of Bentonite for the Improvement of Radionuclide Sorption

Seokju Hong, Jueun Kim, and Wooyong Um*
Pohang University of Science and Technology, 77, Cheongam-ro, Nam-Gu, Pohang-si, Gyeongsangbuk-do 37673, Republic of Korea

(Received October 11, 2021 / Revised November 24, 2021 / Approved December 1, 2021)

Bentonite is the most probable candidate to be used as a buffer in a deep geological repository with high swelling properties, hydraulic conductivity, thermal conductivity, and radionuclide sorption ability. Among them, the radionuclide sorption ability prevents or delays the transport of radionuclides into the nearby environment when an accident occurs and the radionuclide leaks from the canister, so it needs to be strengthened in terms of long-term disposal safety. Here, we proposed a surface modification method in which some inorganic additives were added to form NaP zeolite on the surface of the bentonite yielded at Yeonil, South Korea. We confirmed that the NaP zeolite was well-formed on the bentonite surface, which also increased the sorption efficiency of Cs and Sr from groundwater conditions. Both NaP and NaX zeolite can be produced and we have demonstrated that the generation mechanism of NaX and NaP is due to the number of homogeneous/heterogeneous nucleation sites and the number of nutrients supplied from an aluminosilicate gel during the surface modification process. This study showed the potential of surface modification on bentonite to enhance the safety of deep geological radioactive waste repository by improving the radionuclide sorption ability of bentonite.

Keywords: Bentonite, Surface modification, NaP zeolite, Sorption efficiency, Deep geological repository

*Corresponding Author.
Wooyong Um, Pohang University of Science and Technology, E-mail: wooyongum@postech.ac.kr, Tel: +82-54-279-9563

ORCID

Seokju Hong	http://orcid.org/0000-0002-6685-4442	Jueun Kim	http://orcid.org/0000-0003-2836-4140
Wooyong Um	http://orcid.org/0000-0002-3826-0030		

1. Introduction

Spent nuclear fuel (SNF) is a nuclear fuel material generated after being used in commercial or research reactors and belonged to the high-level radioactive waste. Since the spent nuclear fuels emit a lot of decay heat and radiations, they are currently being stored at dry/wet temporary storage facilities in the nuclear power plant site and will be eventually disposed of at a deep geological repository. Currently, Korea has a plan to build a deep geological repository located hundreds of meters deep underground with horizontal disposal tunnels, vertical disposal holes from the floor of the tunnel, the canister containing high-level radioactive waste, and an engineering buffer material [1]. This buffer material should have some thermal-hydraulic-mechanical (THM) properties [2] such as low hydraulic conductivity, swelling properties, high thermal conductivity, etc. Therefore, bentonite, which has all of these aforementioned properties, has emerged as a promising candidate for the buffer materials of the high-level waste repository.

Bentonite is a clay substance that mainly contains montmorillonite mineral, with excellent swelling properties and high cation exchange capacity (CEC) [3]. The swelling properties and high CEC of the bentonites result from the mineral structure of montmorillonite. Montmorillonite has a 2:1 layer structure with one octahedral sheet of alumina between two tetrahedral sheets of silica. In this structure, the interlayer charge becomes unbalanced due to the isomorphic substitution in which Al^{3+} is replaced with Mg^{2+} in the octahedral site. Thus, the charge balance can be achieved by attracting surrounding cations, and this is the reaction mechanism of cation sorption. The sorbed cations can be hydrated upon contact with water and can increase the gap between the montmorillonite layer bound with relatively weak Van der Waals forces, causing to swell when the montmorillonite reacts with water. In particular, Na-montmorillonite [4] has a higher swelling property than Ca-montmorillonite [5], and most of the bentonite produced in Korea is mainly composed of Ca-montmorillonite [6].

When the bentonite buffer material contacts with groundwater, it gives swelling pressure to the outer wall due to its swelling properties and can block groundwater flowing from the surrounding rock by sealing the pores and cracks present in the disposal hole and host rock. However, excessive swelling pressure can also damage the integrity of the host rock and canister [2]. In general, bentonite is often molded in the form of compressed bentonite block [7] to be used as a buffer material for the high-level waste repository, and when the dry density of compressed bentonite block is high, the swelling pressure can also increase significantly. For this reason, several countries have mixed bentonite and other additive materials to prevent excessive swelling pressure and improve other THM performance properties [8].

For example, in order to reduce the swelling pressure and increase the thermal conductivity, 30wt% of sand was mixed with bentonite in Japan [9], and 50wt% of sand was mixed with bentonite in Canada [4]. Similarly, in Belgium [10], there was a study to increase thermal conductivity by mixing sand and graphite with bentonite. Also, there are some researches about improving the performance of bentonite by mixing additives in Korea. Kim et al. [11] added organic substances such as super absorbent polymer and sodium carboxyl-methyl cellulose to the bentonite to increase the swelling properties. Lee et al. [12] added carbon-nanotube, graphite, alumina, CuO, and Fe_2O_3 into bentonite to increase the thermal conductivity. Especially, they used several different methods to mix additives, including dry hand mixing, wet milling mixing, and dry ball mill mixing, and actually, homogeneous mixing of additives is an important issue in the production of mixed bentonites. In addition to physical mixing, several chemical studies have been conducted for surface modification using organic materials such as surfactants [13, 14]. However, due to the limit of using organic material in the repository, practical application of modified bentonite using organic surfactant may be difficult in a high-level waste repository [15, 16].

In this study, we established an inorganic synthesis

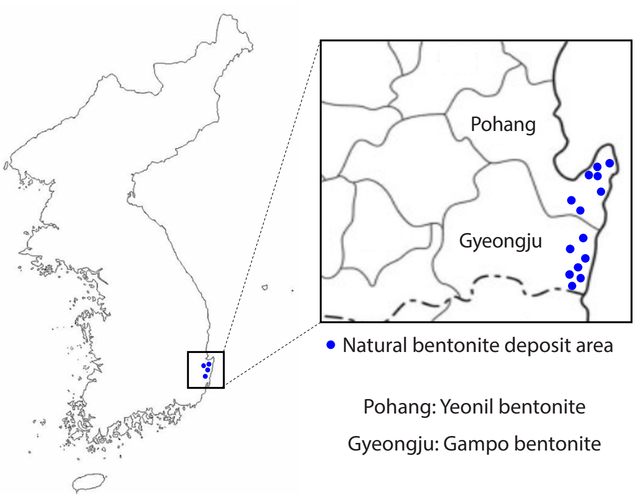

Fig. 1. Domestic natural bentonite production site.

Table 1. Chemical composition of Yeonil Bentonite

Composition	wt%
SiO_2	48.89
Al_2O_3	22.55
Fe_2O_3	6.10
TiO_2	1.39
MgO	1.71
CaO	1.95
Na_2O	1.01
K_2O	1.03
P_2O_5	0.09
L.O.I.	14.62
Total	99.34

method to modify the surface of bentonite to form NaP zeolite to improve the radionuclide removal efficiency and be used as a homogeneous mixing additive with bentonite. The NaP zeolite has a gismondine framework and smaller pores than Faujasite (FAU), Linde type A (LTA), and Mobil type five (MFI) zeolites [17]. Furthermore, NaP zeolite has an excellent radionuclide sorption efficiency based on a high CEC [18] and the organic template is not needed in the manufacturing process, making it a suitable substance for practical use as a buffer material for the high-level waste repository. This study showed the synthetic method and transformation mechanism from bentonite to NaP zeolite with characteristics of original bentonite and Na-P zeolite modified bentonite (NaP/bentonite composite) and the enhanced radionuclides removal efficiencies.

2. Materials & Methods

2.1 Preparation of Korean Natural Bentonite

Yeonil bentonite (produced in Pohang) and Gampo bentonite (produced in Gyeongju) are the representative natural bentonite produced in Korea (Fig. 1). Natural Yeonil bentonite ore was obtained from the Korean Institute of Geoscience and Mineral Resources (Daejeon, Korea) and was ground below 200 mesh (aperture size of 75 μm). To determine the type of Yeonil bentonite, XRF chemical composition analysis (Table 1) was conducted and the results showed that Yeonil bentonite contains more Ca than Na. In addition, the content of Fe_2O_3 is quite high (~6.1wt%) because saponite and nontronite belonged to the same phyllosilicate-smectite group are often coexisting with montmorillonite.

2.2 Surface Modification of Bentonite

For the surface modification of bentonite, sodium hydroxide (SH, NaOH), sodium aluminate (SA, $NaAlO_2$), and sodium metasilicate (SS, Na_2SiO_3) were purchased from Sigma-Aldrich were used without any further processes. The flow chart of the NaP/bentonite composite synthesis method is shown in Fig. 2; First, add 0.16 g of sodium hydroxide and 0.654 g of sodium aluminate into 20 mL of D.I. water to make SA solution, and prepare 1.856 g of sodium silicate into another 20 mL of D.I. water to make SS solution; Put SA solution into a glass beaker, add bentonite (0–9 g), and stir at 300 rpm with a magnetic agitator; Put

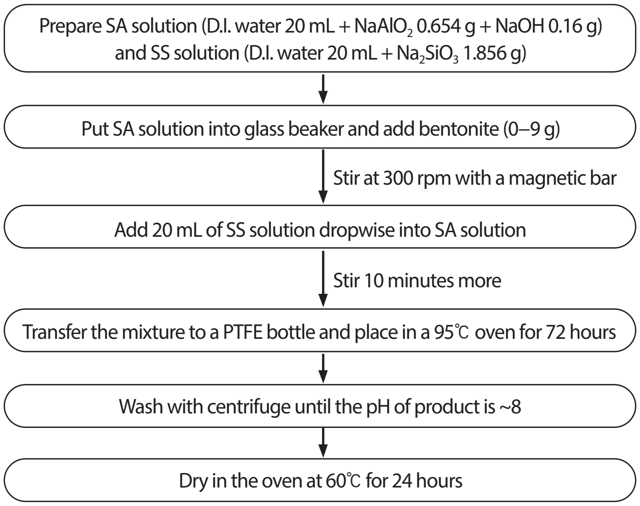

Fig. 2. Flow chart of NaP/bentonite composite synthesis.

Table 2. Characterization and major component of groundwater

	Groundwater	Unit
pH	7.55	-
DO	1.77	mg·L^{-1}
EC	273.3	uS·cm^{-1}
ORP	219.8	mV
TOC	0.463	ppm
Na^+	19.90	mg·L^{-1}
K^+	2.133	mg·L^{-1}
Mg^{2+}	6.043	mg·L^{-1}
Ca^{2+}	11.03	mg·L^{-1}
$Si_{(aq)}$	19.79	mg·L^{-1}
F^-	0.074	mg·L^{-1}
Cl^-	13.43	mg·L^{-1}
Br^-	0.893	mg·L^{-1}
NO_{3-}	0.984	mg·L^{-1}
SO_4^{2-}	27.68	mg·L^{-1}

the mixture in a PTFE (poly-Teflon) bottle and place it in a 95ºC oven for 72 hours. After the reaction, solid products were washed with D.I. water until the pH became ~ 8. After washing, the solid products were used after drying for 24 hours in a 60ºC oven. The synthesis method was originated from our previous study [18], which developed an alkali hydrothermal method that allows NaP zeolite to be crystallized on the surface of the aluminosilicate minerals.

2.3 Characterization

Powder X-ray diffraction (XRD) measurements were conducted using a Rigaku-Miniflex 600 diffractometer operated at 40 kV and 15 mA in the 2Θ range of 5° to 75° at a 0.02° size step using a Cu Kα radiation source. The chemical compositions of the bentonite and NaP/bentonite composites were analyzed by X-ray fluorescence (XRF) measurements with the Bruker S4 Explorer. Fourier-transform infrared (FT-IR) spectra were acquired using a Thermo Fisher Scientific–Nicolet iS 10 spectrometer with 32 scans measured between 550 cm^{-1} and 3,800 cm^{-1} at 4 cm^{-1} increments to analyze the chemical bonding changes in bentonite and NaP/bentonite composites. In order to obtain the pore properties of bentonite and NaP/bentonite composites, both materials were analyzed via N_2 adsorption/desorption isotherms measured at 77K using a BELSORP mini II. Before measurements, the solid samples were degassed under a vacuum for 12 h at 373K. The specific surface area and the pore size distribution were determined by Brunauer Emmett Teller (BET) method and Barrett Joyner Halenda (BJH) equation, respectively. A scanning electron microscope (SEM - JSM 7800F PRIME), coupled with an energy-dispersive spectrometer, was operated at 1 kV to observe the crystalline morphology and any elemental variations of the bentonite and NaP/bentonite composites.

2.4 Batch Sorption Test

For the batch sorption tests, cesium nitrate ($CsNO_3$) and strontium nitrate ($Sr(NO_3)_2$) were used as surrogates for ^{137}Cs and ^{90}Sr. These chemicals were individually added to groundwater to produce Cs and Sr solutions with an initial concentration of 100 ppm and the solid to solution ratio were fixed at 100 (40 mL of solution / 0.4 g of sorbent).

Table 3. Different polymorphs of NaP zeolite

Crystal name	Crystal system	Space group	Unit cell content
Na-P1	cubic	I4	$Na_6Al_6Si_{10}O_{32}\cdot 12H_2O$
Na-P2	orthorhombic	Pnma	$Na_4Al_4Si_{12}O_{32}\cdot 14H_2O$
High Si NaP	tetragonal	$I4_1$/amd	$Na_{3.6}Al_{3.6}Si_{12.4}O_{32}\cdot 14H_2O$
High Al NaP	monoclinic	C2/c	$Na_8Al_8Si_8O_{32}\cdot 15.2H_2O$

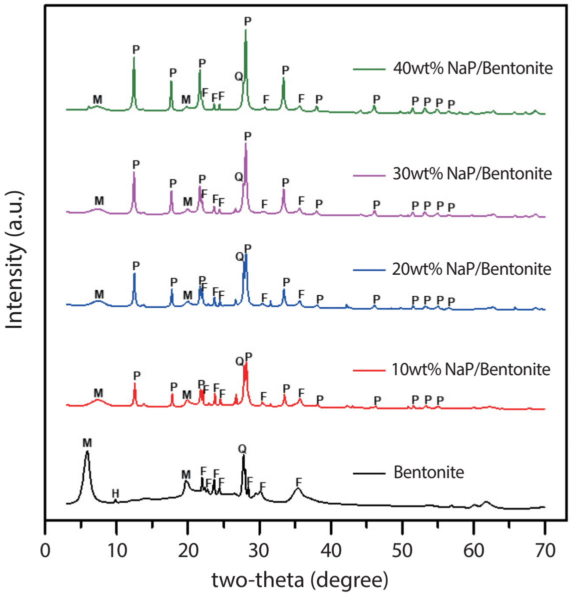

Fig. 3. Synthesis of various NaP/Bentonite composites; Q: quartz, M: montmorillonite, F: Feldspar, H: Halloysite, P: NaP zeolite.

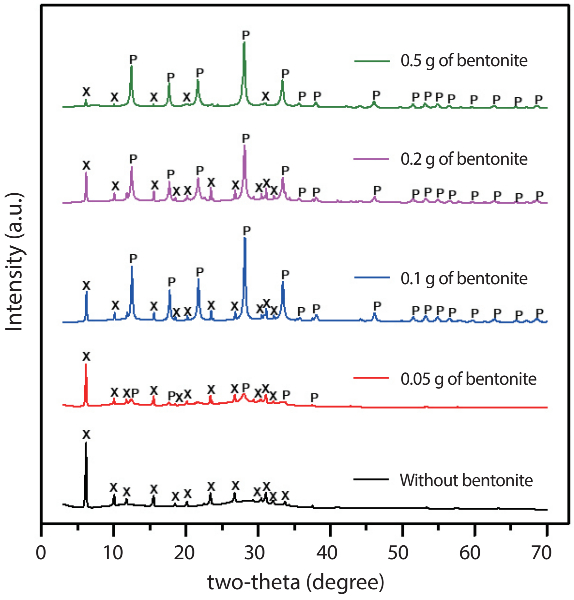

Fig. 4. Variation of NaP and NaX formation with a variation of bentonite mass; X: NaX zeolite, P: NaP zeolite.

We used the groundwater obtained from Gyeongju radioactive waste repository site, and the characterization of the groundwater is shown in Table 2.

The removal efficiency of Sr or Cs, R(%) was calculated using Eq. (1),

$$R\ [\%] = \frac{C_i - C_f}{C_i} \times 100 \qquad (1)$$

where C_i and C_f are the initial and final concentration of radionuclide (Sr or Cs) in solution, respectively. Since both NaP zeolite [19] and bentonite [20] reach equilibrium with Cs and Sr within 3 days, batch sorption tests were conducted in duplicate for 7 days at room temperature.

3. Results & Discussions

3.1 Synthesis of NaP/bentonite Composites

To modify the bentonite surface with NaP zeolite, we tried to synthesize the NaP/bentonite composites by changing the proportion of NaP zeolite. Different diffraction patterns depending on the proportion of NaP zeolite added to bentonite are described in Fig. 3. In original Yeonil bentonite, we could observe not only peaks of montmorillonite (two-theta of 5.9° and 19.8°), but also the peaks of quartz (two-theta of 27.8°), halloysite (two-theta of 9.9°), and various feldspar (mostly anorthite) minerals. Even after the

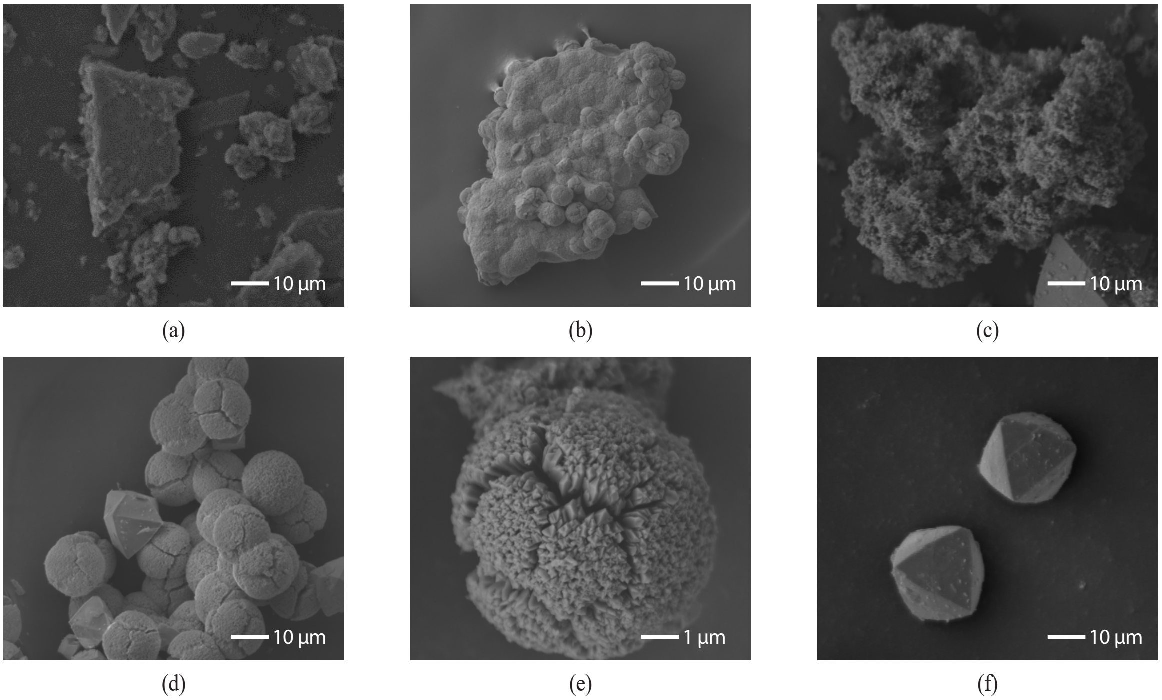

(a) (b) (c) (d) (e) (f)

Fig. 5. Scanning electron microscope images of crystals. (a) bentonite, (b) formation of NaP zeolite on the bentonite surface, (c) amorphous alumino-silicate gel, (d) Mix of NaP and NaX zeolite crystals, (e) Spherical NaP zeolite cluster, (f) Octahedral NaX zeolite crystal.

surface modification reaction, some mineral phases such as montmorillonite, quartz, and feldspar have still remained.

Especially, montmorillonite's characteristic peak (two-theta of 5.9º) undergoes two major changes after the synthesis reaction, regardless of the proportion of NaP zeolite. First, the aforementioned montmorillonite peak was shifted from 5.9º to 7.3º, because the original bentonite, previously present as Ca-bentonite was ion-exchanged to Na-bentonite due to a large number of sodium ions present in the synthetic solutions (SA, SH, and SS). Hiroshi et al. [21] demonstrated that Na-montmorillonite (12.96 Å) has a smaller interlayer distance than Ca-montmorillonite (15.72 Å). Second, the intensity of the peak was greatly reduced because the NaP zeolite was formed to coat the surface of the bentonite while some Si in the montmorillonite was dissolved in high pH conditions.

The NaP zeolite has a gismondine (GIS) framework topology and has some polymorphs depending on Si/Al ratio [22]. Several different polymorphs of NaP zeolites are summarized [23-26] in Table 3. From the diffraction analysis results, our NaP zeolite produced on the surface of the bentonite was identified as Na-P1 zeolite, specifically.

3.2 Mechanism of NaP Formation on the Surface-modified Bentonite

In this study, we used a method of mixing bentonite with 20 mL of SA solution followed by adding 20 mL of SS solution to modify the surface of the bentonite. However, if the bentonite was not added while proceeding with the same synthesis method shown in Fig. 2, NaX zeolite of the FAU type was produced, not NaP zeolite of the GIS type. Therefore, in order to identify the mechanism of surface modification, the synthesis mechanism of NaP and NaX zeolite must be investigated first. Through the diffraction pattern in Fig. 4, we can see that the formation of NaP and

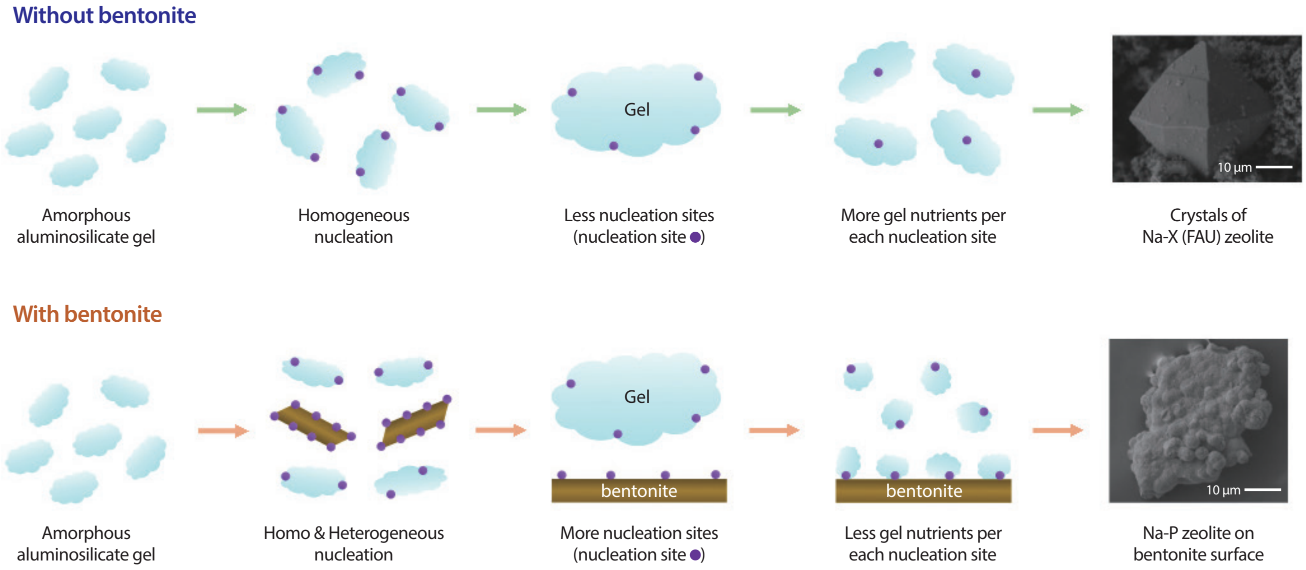

Fig. 6. Crystallization of aluminosilicate gel and surface modification mechanism.

NaX depends on the added amount of bentonite. If bentonite was not added at all, we could observe that only NaX zeolite was formed, and as the amount of added bentonite increased, the formation of NaX decreased while the amount of NaP zeolite increased.

The formation variations of NaP and NaX zeolite were also observed through the SEM images (Fig. 5). Original bentonite has a flat plate shape and a relatively smooth surface morphology (Fig. 5(a)). On the other hand, the surface-modified bentonite (10wt% NaP/bentonite, Fig. 3) had a surface that was covered with spherical NaP zeolite, as shown in Fig. 5(b). This surface modification was well achieved when the initial amount of added bentonite was enough. However, if the amount of added bentonite is insufficient, the amorphous aluminosilicate gel (Fig. 5(c)) can crystallize into not only NaP zeolite but also NaX zeolite (Fig. 5(d)). The NaP zeolite has a diamond-shaped morphology with a spherical cluster as shown in Fig. 5(e), and the NaX zeolite has a bipyramidal octahedron shape as shown in Fig. 5(f).

G. Harvey [27] suggested the concept of supplying Si and Al nutrients to the nucleation process when describing the formation of NaP and NaX zeolite from aluminosilicate gel. When we use polymerized sodium silicate solutions, NaP (type of GIS) zeolite can be easily formed compared to NaX (type of FAU) zeolite because the formation of aluminosilicate gel is slow, and fewer Si and Al nutrients are supplied to the NaP nucleation site. Similarly, our bentonite surface modification can be described with the same mechanism (illustrated in Fig. 6).

First, if there is no bentonite, only the homogeneous nucleation site exists in the synthetic solutions because only water and formation gel are present in the synthetic solution. Aluminosilicate gel supplies Si and Al nutrients to relatively few nucleation sites, so each nucleation site is supplied with sufficient Si and Al. In this case, each nucleus can be crystallized into NaX zeolite. On the other hand, when bentonite is added, water, gel, and some bentonite particles coexist in the synthetic solution. Then, in addition to the existing homogeneous nucleation site, the heterogeneous nucleation site can also exist on the surface of the bentonite particles. At this time, the number

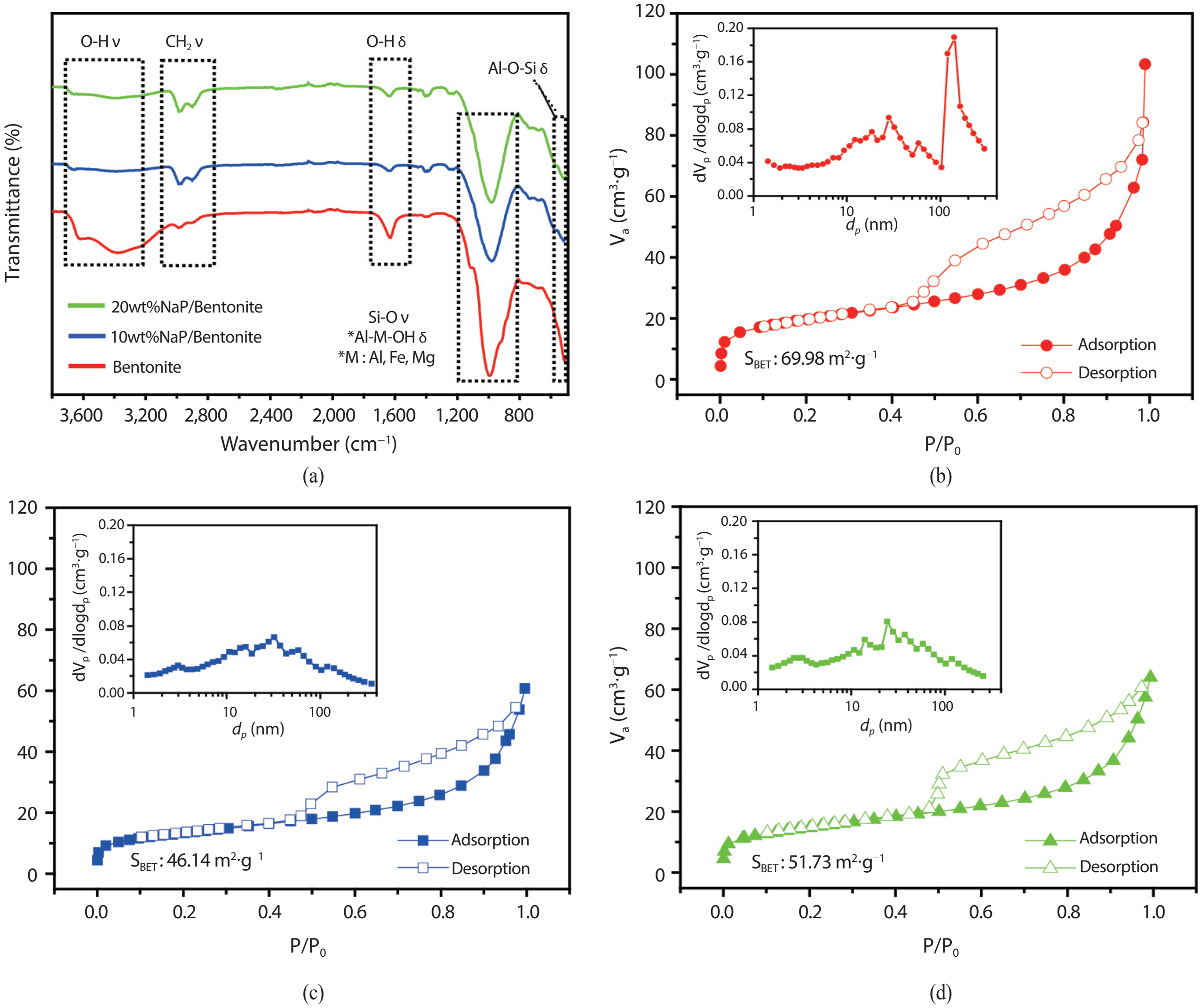

Fig. 7. (a) Infra-red spectra of original bentonite, 10wt% NaP/Bentonite, and 20wt% NaP/Bentonite, N_2 adsorption/desorption isotherms and BJH pore size distributions of (b) original bentonite, (c) 10wt% NaP/Bentonite, and (d) 20wt% NaP/Bentonite.

of nucleation sites has increased, so each nucleation site cannot receive sufficient Si and Al nutrients from the limited source of the synthetic solution. In this case, each nucleus can be crystallized into NaP zeolite on the surface of bentonite, which shows the bentonite covered by NaP zeolite, not NaX zeolite. These results are also very effective in terms of radionuclide sorption because NaP zeolite can remove Cs and Sr better than NaX zeolite in saline conditions [28].

3.3 FT-IR and BET/BJH Pore Analysis of NaP/bentonite Composites

It is expected that the removal efficiency of cationic radionuclides increases if the NaP zeolite content in bentonite increases. However, the reduced content of montmorillonite may result in reduced swelling properties. Therefore, additional experiments were focused on the original bentonite, 10wt% NaP/bentonite, and 20wt% NaP/bentonite. First, FT-IR spectra were obtained to confirm the chemical bond type of original bentonite and NaP/bentonite composites (Fig. 7(a)). From the bentonite IR spectrum, we could see the Al-O-Si bending at 513 cm^{-1} and the Al-Al-OH bending at 918 cm^{-1}, which are the representative peaks of the montmorillonite [29]. In addition, high water content properties and the presence of the hydroxyl group of montmorillonite were confirmed by the OH stretching at 3,615 cm^{-1}, OH vibrational at 3,390 cm^{-1}, and OH bending at 1,631 cm^{-1}. The vibration of CH_2 at peaks of 2,900 cm^{-1} and 2,985 cm^{-1} was observed, which is an indication of organic impurity in natural bentonite [30].

After the bentonite surface modification, IR spectra showed two major changes. First, the OH peaks were significantly reduced, which means that surface modification reduced the number of hydroxyl groups and water contents. Second, the peak of Al-M-OH is hardly distinguished in NaP/bentonite composites. The spectra of original bentonite in the range of 1,000 cm^{-1} to 800 cm^{-1} are slightly different from the spectra of other NaP/bentonite composites due to the three types of Al-M-OH bending peaks present along with Si-O vibrational peak. These peaks are Al-Al-OH at 914 cm^{-1}, Al-Fe-OH at 876 cm^{-1}, and Al-Mg-OH at 833 cm^{-1}, respectively. These peaks can be observed by Al^{3+} isomorphically substituted by Fe^{2+} and Mg^{2+} in bentonite structure. However, these peaks become difficult to distinguish after the NaP zeolite surface modification.

The pore analysis also showed that the original bentonite, 10wt% NaP/bentonite, and 20wt% NaP/bentonite were porous solid materials with clear hysteresis (Figs. 7(b), 7(c), and 7(d)). Original bentonite showed the highest specific surface area (S_{BET}) of 69.98 $m^2 \cdot g^{-1}$, while 10wt% NaP/bentonite and 20wt% NaP/bentonite showed lower values of specific surface area like 46.14 $m^2 \cdot g^{-1}$ and 51.73 $m^2 \cdot g^{-1}$, respectively. According to the BJH pore size distribution plot, macropores larger than 100 nm disappeared after the surface modification, suggesting that S_{BET} of NaP/bentonite composites was reduced compared to the original bentonite. One more, the S_{BET} of 20wt% NaP/bentonite is higher than S_{BET} of 10wt% NaP/bentonite because the number of mesopores increased as the amount of NaP zeolite increased.

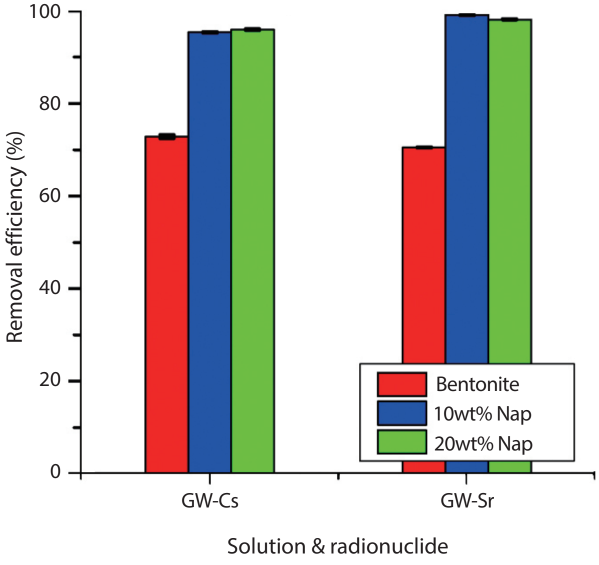

Fig. 8. Batch sorption experiment for the removal of Cs and Sr with different NaP/bentonite composites in groundwater conditions.

3.4 Cs and Sr Removal Efficiency of NaP/bentonite Composites

To confirm the improvement of the cationic radionuclide removal efficiency of NaP/bentonite composites, batch sorption tests were conducted on Cs and Sr, respectively, under the groundwater conditions in Table 2.

The original bentonite showed 72.8% of Cs removal efficiency and 70.5% of Sr removal efficiency. On the other hand, 10wt% NaP/bentonite showed 95.4% of Cs removal efficiency and 99.1% of Sr removal efficiency (Fig. 8). Although the specific surface areas were decreased after the surface modification (Fig. 7), it is evaluated that the overall cationic radionuclide removal efficiency was increased with the formation of NaP zeolite on the bentonite surfaces. Since the 20wt% NaP/bentonite showed almost similar removal efficiency (Cs: 95.9%, Sr: 98.2%) to 10wt% NaP/bentonite (Cs: 95.4%, Sr: 99.1%) in our experimental condition.

As a result, the cation removal efficiency of 10wt% NaP/bentonite composite was improved compared to the original bentonite, and since the content of the NaP zeolite is low (10wt%), it is considered that there would be no critical THM performance degradation compared to the original bentonite.

4. Conclusions

Organotemplate-free hydrothermal synthesis of NaP/bentonite composites was established for the higher cationic radionuclide removal efficiency. At the temperature of 95ºC, sodium metasilicate, sodium aluminate, and sodium hydroxide were used to form NaP zeolite mineral phases on the surface of Korean Yeonil bentonite. From diffraction analysis and SEM images, we confirmed that spherical clusters of NaP zeolite were formed on the surface of bentonite.

If we only added chemicals without bentonite, NaX zeolite tended to be formed instead of NaP zeolite. The added chemicals become aluminosilicate gel in the aqueous phase and this gel supplies Al and Si nutrients enough to provide the nucleation site for forming zeolite crystals. Therefore, without bentonite added, there were only homogeneous nucleation sites and the number of nutrients supplied to each site was sufficient to form NaX zeolite. However, when we added bentonite, the number of nucleation sites increases with the increased sites on the bentonite surfaces and the number of nutrients supplied to each site was insufficient to form NaX zeolite. At this time, on the surface of bentonite, NaP zeolite crystallizes instead of NaX zeolite.

The water content and the presence of macropores of NaP/bentonite composite were reduced compared to the original bentonite and confirmed by FT-IR spectra and BJH analysis. Due to the loss of macropores, NaP/bentonite composite has a smaller specific surface area than the original bentonite. Nevertheless, the NaP/bentonite composite showed better Cs and Sr removal efficiency than the original bentonites. This is because of the presence of the NaP zeolite which has high radionuclide removal efficiency, and it was confirmed that even with only 10wt% of NaP zeolite, the radionuclide removal efficiency was sufficiently improved from 70% to 95%. Based on these results, enhanced cationic radionuclide removal can be prepared by NaP zeolite formed on the surface of bentonite or mixed with bentonite. In addition, additional studies are needed to confirm whether our NaP/bentonite composite, which has improved cation removal efficiency through surface modification, has not significantly degraded the original benefits of THM properties in bentonite.

Acknowledgements

This research was supported by the National Research Foundation of Korea funded by the Ministry of Education (NRF-2021M2E3A2044299).

REFERENCES

[1] J. Lee, D. Cho, H. Choi, and J. Choi, “Concept of a Korean Reference Disposal System for Spent Fuels”, J. Nucl. Sci. Technol., 44(12), 1565-1573 (2007).
[2] W.J. Cho, J.O. Lee, K.S. Chun, and H.S. Park, “Analysis of Functional Criteria for Buffer Material in a High-level Radioactive Waste Repository”, Nucl. Eng. Technol., 31(1), 116-132 (1999).
[3] D. Meyer and J.J. Howard. Evaluation of Clays and Clay Minerals for Application to Repository Sealing, Office of Nuclear Waste Isolation Technical Report, ONWI-486 (1983).
[4] M.N. Gray, S.C.H. Cheung, and D.A. Dixon. The Influence of Sand Content on Swelling Pressures and Structure Developed in Statically Compacted Na-bentonite, Atomic Energy of Canada Limited Report, AECL-7825 (1984).

[5] M.V. Villar and P. Rivas, “Hydraulic Properties of Montmorillonite-quartz and Saponite-quartz Mixture”, Appl. Clay Sci., 9(1), 1-9 (1994).

[6] M. Kim, S. Lee, E. Cheon, M. Kim, and S. Yoon, “Thermochemical Changes on Swelling Pressure of Compacted Bentonite”, Ann. Nucl. Energy, 151, 107882 (2021).

[7] S. Yoon, W.H. Cho, C. Lee, and G.Y. Kim, “Thermal Conductivity of Korean Compacted Bentonite Buffer Materials for a Nuclear Waste Repository”, Energies, 11(9), 2269 (2018).

[8] D.A. Dixon, M.N. Gray, and A.W. Thomas, “A Study of the Compaction Properties of Potential Clay-sand Buffer Mixtures for use in Nuclear Fuel Waste Disposal”, Eng. Geol., 21(3-4), 247-255 (1985).

[9] Japan Nuclear Cycle Development Institute. H12: Project to Establish the Scientific and Technical Basis for HLW Disposal in Japan: Supporting Report 2, JNC Report, JNC TN1410 2000-003 (1999).

[10] ONDRAF/NIRAS. Technical Overview of the SAFIR 2 Report: Safety Assessment and Feasibility Interim Report 2, ONDRAF/NIRAS Report, NIROND 2001-05E (2001).

[11] C.R. Kim, J.H. Kim, W.S. Lyoo, C.W. Joo, and H. Jeon, “Swelling Behavior Evaluation of Bentonite With Additives Mixture”, Text. Sci. Eng., 46(6), 326-333 (2009).

[12] J.P. Lee, H.J. Choi, J.W. Choi, and M. Lee, “Increasing of Thermal Conductivity From Mixing of Additive on a Domestic Compacted Bentonite Buffer”, J. Nucl. Fuel Cycle Waste Technol., 11(1), 11-21 (2013).

[13] S.Y. Lee and S.J. Kim, “Dehydration Characteristics of Cationic Surfactant-Modified Montmorillonite”, J. Miner. Soc. Korea, 15(4), 305-314 (2002).

[14] J.B. Kim, “The Study for Removal of As by the OTA-Br-impregnated Bentonite Adsorbent”, KSWST Jour. Wat. Treat., 26(1), 55-67 (2018).

[15] Svensk Kaernbraenslefoersoerjning AB, Final Storage of Spent Fuel – KBS-3, Swedish Nuclear Fuel and Waste Management Company, Stockholm (1983).

[16] L.H. Johnson, J.C. Tait, D.W. Shoesmith, J.L. Crosthwaite, and M.N. Gray. The Disposal of Canada’s Nuclear Fuel Waste: Engineered Barriers Alternatives, Atomic Energy of Canada Limited Report, AECL-10718 (1994).

[17] P. Sharma, J.S. Song, M.H. Han, and C.H. Cho, “GIS-NaP1 Zeolite Microspheres as Potential Water Adsorption Material: Influence of Initial Silica Concentration on Adsorptive and Physical/topological Properties”, Sci. Rep., 6, 22734 (2016).

[18] S. Hong and W. Um, “Top-Down Synthesis of NaP Zeolite From Natural Zeolite for the Higher Removal Efficiency of Cs, Sr, and Ni”, Minerals, 11(3), 252 (2021).

[19] H. Mimura and K. Akiba, “Adsorption Behavior of Cesium and Strontium on Synthetic Zeolite P”, J. Nucl. Sci. Technol., 30(5), 436-443 (1993).

[20] R. Wang, Y. Chu, and M. Chen, “Adsorption Kinetics of $^{137}Cs^+/^{90}Sr^{2+}$ on Ca-Bentonite”, Water Environ. Res., 89(9), 791-797 (2017).

[21] H. Tetsuka, I. Katayama, H. Sakuma, and K. Tamura, “Effects of Humidity and Interlayer Cations on the Frictional Strength of Montmorillonite”, Earth Planets Space, 70, 56 (2018).

[22] Z. Huo, X. Xu, Z. Lü, J. Song, M. He, Z. Li, Q. Wang, and L. Yan, “Synthesis of Zeolite NaP With Controllable Morphologies”, Microporous Mesoporous Mater., 158, 137-140 (2012).

[23] U. Håkansson, L. Fälth, and S. Hansen, “Structure of a High-silica Variety of Zeolite Na-P”, Acta Cryst. C46, 1363-1364 (1990).

[24] Ch. Baerlocher and W.M. Meier, “The Crystal Structure of Synthetic Zeolite Na-P1, an Isotope of Gismondine”, Z. Kristallogr. Cryst. Mater., 135(S), 339-354 (1972).

[25] S. Hansen, U. Håkansson, A.R. Landa-Canovas, and L. Falth, “On the Crystal Chemistry of NaP Zeolites”, Zeolites, 13(4), 276-280 (1993).

[26] B.R. Albert, A.K. Cheetham, J.A. Stuart, and C.J. Adams, “Investigations on P Zeolites: Synthesis, Characterization, and Structure of Highly Crystalline low-silica NaP”, Microporous Mesoporous Mater., 21(1-3), 133-142 (1998).

[27] G. Harvey and L.S. Dent-Glasser, “Structure and Properties of Aluminosilicate Solutions and Gels”, in: Zeolite Synthesis, vol. 398, 49-65, American Chemical Society, Washington DC (1989).

[28] M.W. Munthali, E. Johan, H. Aono, and N. Matsue, “Cs^+ and Sr^{2+} Adsorption Selectivity of Zeolites in Relation to Radioactive Decontamination”, J. Asian Ceram. Soc., 3(3), 245-250 (2015).

[29] M. Hayati-Ashtiani, “Characterization of Nano-Porous Bentonite (Montmorillonite) Particles Using FTIR and BET-BJH Analyses”, Part. Part. Syst. Charact., 28(3-4), 71-76 (2011).

[30] U.O. Aroke, A. Abdulkarim, and R.O. Ogubunka, “Fourier-transform Infrared Characterization of Kaolin, Granite, Bentonite, and Barite”, ATBU J. Environ. Technol., 6(1), 42-53 (2013).